TOUGHNESS DUE TO HYSTERETIC DEFORMATION

This topic is an active area of research. Here I describe some aspects using examples.

Andrews (1963) perhaps is the earliest paper that articulated the effect of hysteretic deformation on fracture. The title of his paper is "Rupture propagation in hysteresial materials: stress at a notch". Andrews focused on rubber, but hysteresis is important to all tough materials.

A frame-by-frame movie. We have described this movie many times in class.

Frame 1. A crack is cut into a body of a material using a diamond saw. No force is applied to the body yet.

Frame 2. Apply a small load. A small region around the front of the crack yields. This small region is called the *plastic zone*. The body remains elastic outside the plastic zone. The front of the crack remains stationary.

Frame 3. Increase the load slightly. The plastic zone increases in size. The front of the crack still remains stationary.

Frame 4. Increase the load still more. The front of the crack starts to advance. The larger the load, the more the crack advances.

Frame 5. The load reaches a constant level, the front of the crack advances in a steady state. Plastic deformation is confined in the thin layers beneath the crack surfaces. The thickness of the plastic layers remains constant as the front of the crack advances.

Work done in the steady state. Let us focus on Frame 5. The load reaches a constant level, the front of the crack advances in a steady state. Plastic deformation is confined in the thin layers beneath the crack surfaces. The thickness of the plastic layers remains constant as the crack advances.

Follow a material particle near the plane of the crack. As the front of the crack passes by, the deformation of the material particle undergoes hysteresis: elastic loading, plastic flow, and then elastic unloading. Sketch the stress-strain curve of a material particle. When the front of the crack is at a particular location, the stress acting on the material particle is σ_{ij}. Associated with a small advance of the crack, the strain of the material particle changes by $d\varepsilon_{ij}$, and the work done by the stress is $\sigma_{ij} d\varepsilon_{ij}$. As the crack advances, the material particle is initially far ahead the front of the crack, and finally far behind the front of the crack; the material particle going through a history of stress and strain. The work done by the entire history of stress on the material particle is

$$W = \int \sigma_{ij} d\varepsilon_{ij} .$$

The integral is over the entire loading-unloading history of the material particle. Note that W is the work per unit volume.

This above work is the same for all material particles at the same height y from the plane of the crack, but varies as a function $W(y)$. For a material particle outside the plastic layer

$$w_p = \int W(y) dy$$

The integral extends from the plane of the crack to the elastic-plastic boundary. The material particle dissipates energy as heat.

Of course, we cannot calculate this integral until we determine the history of the stress and strain by solving a sequence of boundary-value problems as the front of the crack advances. This capability has become widely available in recent decades, as many research groups become comfortable with sophisticated finite element software.

Stress-assisted Transformation in Zirconia

Ceramic steel (Garvie et al., 1975). When ZrO_2 is lightly doped with Y_2O_3, the tetragonal lattice can be metastable at the room temperature. Under stress, the tetragonal phase can transform to the monoclinic phase. The crystals of the two phases have different lattice constants. Consequently, the transformation is accompanied with a change in strain. Sketch the stress-strain diagram. Identify the critical stress, the transformation strain, and hysteresis.

Toughening mechanism. Particles of tetragonal ZrO_2 in a Al_2O_3 matrix. Pre-cut crack. When the crack grows, the ZrO_2 particles transform from the tetragonal phase to the monoclinic phase. Dissipation. No crack-tip blunting. R-curve.

The model. (McMeeking and Evans, 1982; Budiansky, Lambropoulos, and Hutchinson, 1983). Let H be the thickness of the zone of the transformation. The zone of transformation is small compared to the specimen and the length of the crack a. That is, we assume small-scale transformation.

In the annulus $H < r < a$, the stress field is given by the square-root singular field:

$$\sigma_{ij}(r,\theta) = \frac{K_{\text{appl}}}{\sqrt{2\pi r}} f_{ij}(\theta),$$

where the stress intensity factor K_{appl} represents the amplitude of the applied load.

The tip of the crack is atomistically sharp. Let b be the atomic dimension. In the annulus $b < r < H$, the stress field is also given by the square-root singular field:

$$\sigma_{ij}(r,\theta) = \frac{K_{\text{tip}}}{\sqrt{2\pi r}} f_{ij}(\theta).$$

where the stress intensity factor K_{tip} represents the amplitude of the local field.

The phase transformation tends to close the crack, so that

$$K_{\text{appl}} > K_{\text{tip}}.$$

When the crack extends, atomic bonds break at the tip of the crack, so that K_{tip} reaches the toughness of the ceramics without transformation. The applied load, however, scales with K_{appl}. Transformation is said to shield the tip of the crack from the applied load. The ratio $K_{\text{appl}} / K_{\text{tip}}$, knows as the shielding factor, quantifies toughening due to transformation.

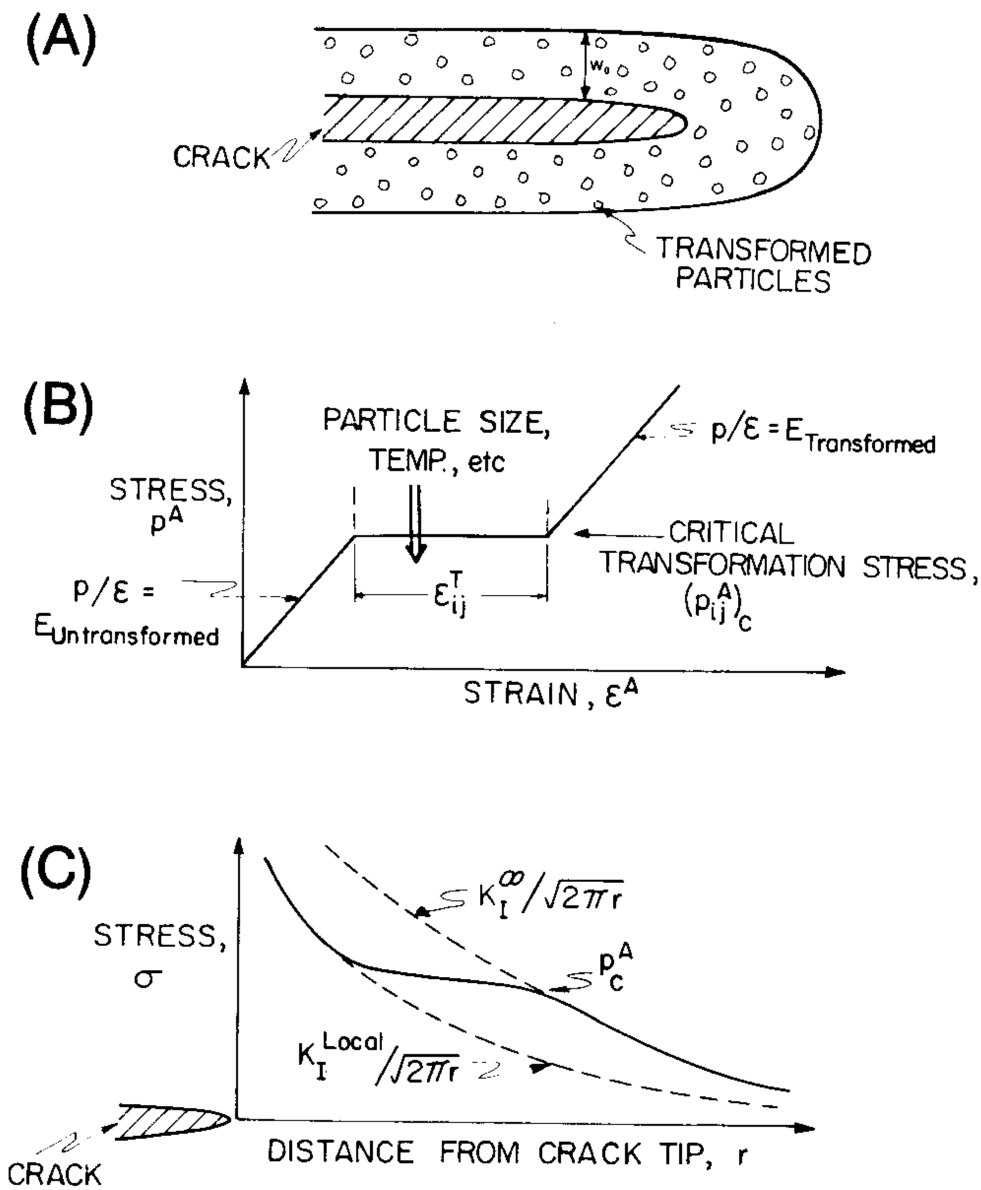

Fig. 1. (*A*) Schematic of a transformation zone around a crack induced by the martensite transformation of particles. (*B*) Typical stress-strain behavior for a martensite transformation; e_{ij}^T is the unconstrained transformation strain and p_{ijc}^A the critical stress needed to induce transformation (which depends on e.g. particle size). Note the linearity of the stress/strain relation for stresses in excess of the transformation stress. (*C*) Stress field ahead of a crack tip, as modified by a transformation zone.

The toughening ratio can be calculated by solving the boundary value problem. However, the scaling of the solution may be understood from the following considerations. The thickness of the zone of transformation can be estimated in a similar way as that of the plastic zone, namely,

$$H = \alpha \left(\frac{K_{\text{appl}}}{\sigma_c} \right)^2 ,$$

where σ_c is the critical stress for transformation, and α is a dimensionless number.

The local stress intensity factor K_{tip} is due to two effects: the opening caused by the applied load, and closing caused by transformation. A linear superposition gives that

$$K_{\text{tip}} = K_{\text{appl}} - \beta E \varepsilon^T \sqrt{H} ,$$

where ε^T is the strain associated with transformation, and β is a dimensionless number.

Eliminating H from the above relations, we obtain the shielding factor,

$$\frac{K_{\text{appl}}}{K_{\text{tip}}} = \frac{1}{1 - \beta \sqrt{\alpha} \dfrac{E \varepsilon^T}{\sigma_c}} .$$

This model indicates several trends:

- K_{tip}
- ε^T
- σ_c

Rubber-Modified Epoxy

The similar concept is applied applicable to some other material systems, such as rubber-modified epoxy (Du et al., 1998). Briefly describe the phenomenon.

Tough and Stretchable Hydrogels

Briefly describe the phenomenon (Gong, 2003; Sun et al, 2012).

Plastic Deformation in Metals

Needleman (1987). Recall the basic processes accompanying fracture:

facture = deformation + separation

For metals, the two processes—deformation and separation—correspond to two groups of actors:

- Deformation: dislocation plasticity, stress-assisted phase transition, or twining.
- Separation: breaking atomic bonds (cleavage), or growing voids.

Rather than describing these actors in detail, Needleman (1987) represented them using two known models:

▪ Deformation is represented by continuum plasticity. Parameters: $\sigma_0, \varepsilon_0, \alpha, n$

- Separation process is represented by a traction-separation relation (i.e., a crack-bridging or cohesive zone model), $\sigma(\delta)$. Parameters: σ_B, Γ_B.

For the first time, Needleman (1987) included both the body separation process and deformation hysteresis in a single boundary value problem. This combination of two models has made huge impact in the field.

Two figures taken from Suo and Shih (1993). Describe the two figures.

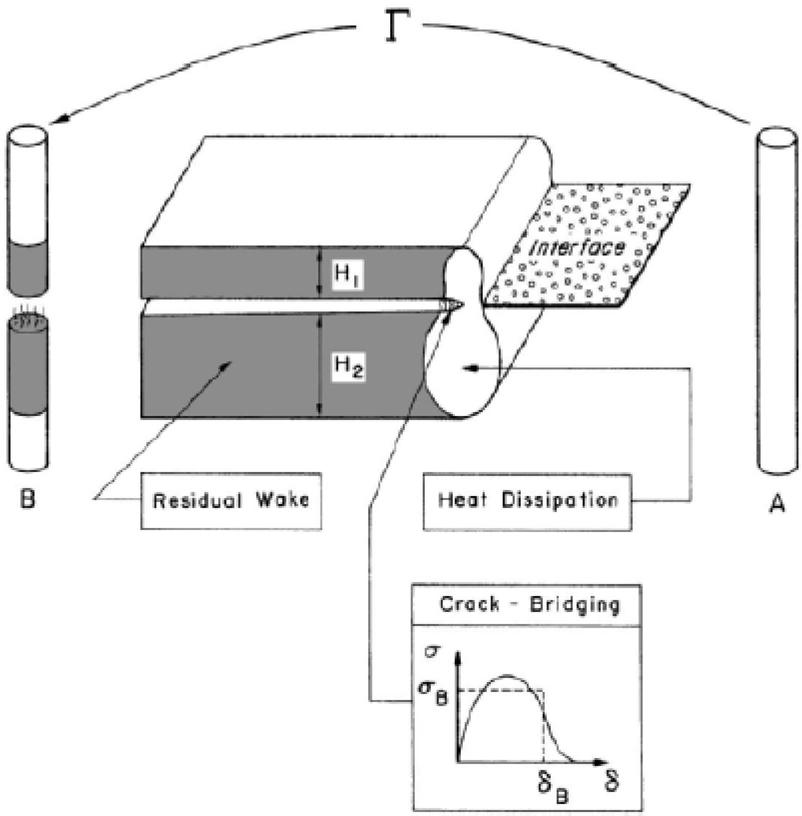

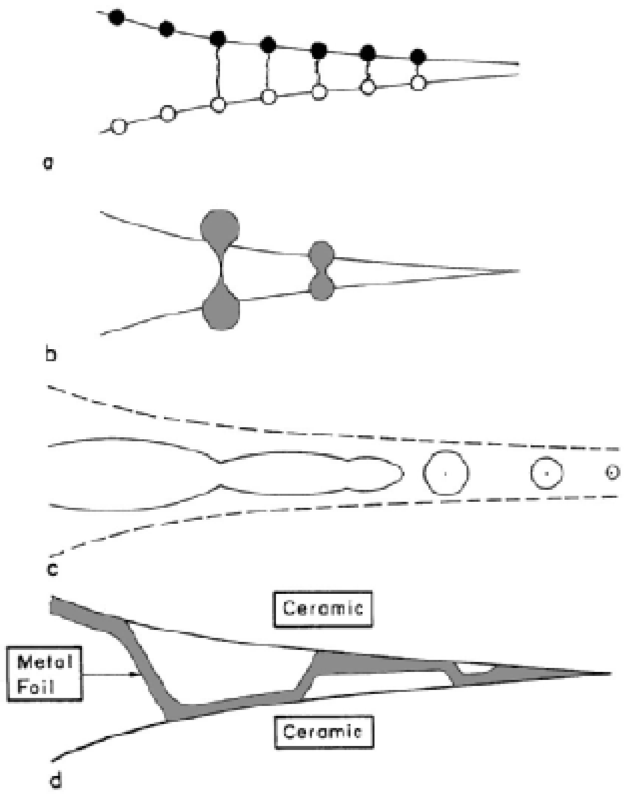

Figure 12.11. Crack-bridging mechanisms: (a) atomic adhesion, (b) ductile ligaments, (c) hole growth, and (d) alternating debonding.

Compute R-curve under the small scale yielding conditions (Tvergaard and Hutchinson, 1992). Assume the small scale yielding condition. Consequently, consider a semi-infinite crack. The plastic zone size is finite. Remote from the crack tip, the material is elastic. Prescribe the external boundary condition by the *K*-field,

$$\sigma_{ij}(r,\theta)=\frac{K}{\sqrt{2\pi r}}\Sigma_{ij}(\theta).$$

The field prevails at a distance *r* much larger than the plastic zone size. The parameter *K* represents the load level.

On the size scale much larger than the plastic zone size, we can neglect the plastic zone size, and treat the plastic zone as a mathematical point. In particular, we can speak of the energy release rate, *G*, the elastic energy reduction associated with the crack advancing by a unit area.

The plastic zone size. Recall Irwin's relation:

$$G=\frac{K^2}{E}.$$

We can either use *K* or *G* to indicate the level of the external load. Also recall the plastic zone size $r\sim(K/\sigma_o)^2$. The model has one length scale: the plastic zone size at the onset of crack growth, namely

$$R_o = \frac{\Gamma_B}{3\pi\sigma_o\varepsilon_o}$$

The factor 3π is introduced by convention.

The *R*-curve. Draw a growing crack, with body separation and deformation hysteresis. Draw a *R*-curve. Before the bridging zone start to unload, the material does not unload and behaves like a nonlinear elastic material. Consequently, the *J*-integral is path-independent, so that the external load is directly linked to the traction-separation relation as

$$G = \int_o^{\delta_{tail}} \sigma(\delta) d\delta$$

As the external load increases, the plastic zone size increases, and the bridging zone tail opening increases. The crack tip remains more or less stationary.

After the bridging zone unloads in the tail, and extends at the tip, the crack starts to advance significantly. The material in the background starts to unload. The *J*-integral becomes path-dependent, and *G* exceeds Γ_B. The full *R*-curve can be calculated from the model.

The steady-state fracture energy, Γ_{SS}, can also be calculated from the model.

$$\frac{\Gamma_{ss}}{\Gamma_B} = f\left(\frac{\sigma_B}{\sigma_o}, n, \alpha, \varepsilon_o\right).$$

The steady-state plastic zone size

$$R_{SS} = \frac{\Gamma_{SS}}{3\pi\sigma_o\varepsilon_o}.$$

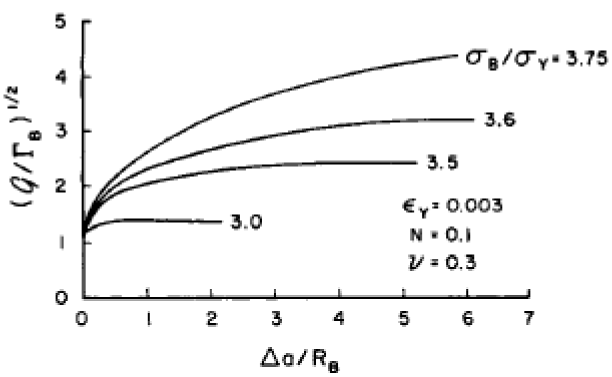

Figure 12.12. Fracture resistance curve resulting from background plasticity shielding. *(From Tvergaard and Hutchinson 1992.)*

The model is applicable in a narrow region. For example, consider the nonhardening material. If $\sigma_B / \sigma_o < 2$, the bridging is too weak, and the background plasticity contributes negligibly to the fracture energy.

If $\sigma_B / \sigma_o > 3$, the bridging is too strong, and the fracture energy becomes infinite. The latter is expected from the McMeeking solution. When the bridging strength is high, the crack tip blunts, and the stress level at the crack tip is about a few times of the yield strength, insufficient to break the bridging.

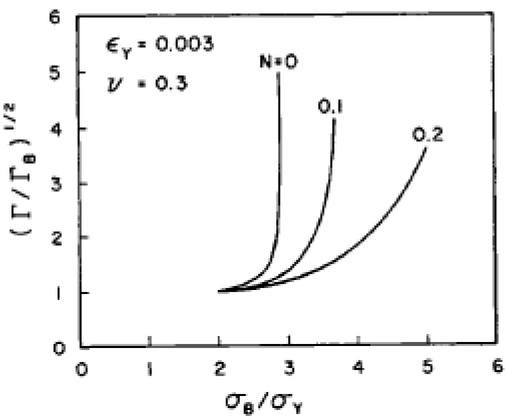

Figure 12.13. Steady-state shielding ratio as a function of bridging strength relative to yield strength. *(From Tvergaard and Hutchinson 1992.)*

Suo, Shih and Varias (1993). Experimental observations of cleavage in the presence of plastic flow. Metal-ceramic interface. Environmental attack. Typically, the cohesive strength is much higher than the yield strength.

Plasticity is a discrete process. Dislocation spacing is much larger than atomic spacing. D

Assume the crack tip does not emit dislocation. Crack is atomistically sharp.

Within size D, the material is elastic. Elastic cell.

Estimate stress change in the elastic cell.

The model. Fracture process is described by cleavage, fracture energy Γ_o. The deformation process is described by continuum plasticity. A dimensionless parameter:

$$\frac{\Gamma_o}{\sigma_o \varepsilon_o D}.$$

The steady-state fracture energy can be calculated from the model

$$\frac{\Gamma_{ss}}{\Gamma_o} = f\left(\frac{\Gamma_o}{\sigma_o \varepsilon_o D}\right)$$

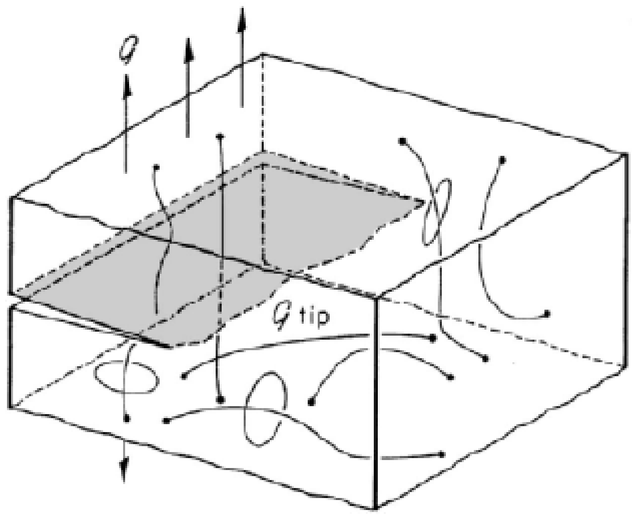

Figure 12.14. A decohesion front in a network of pre-existing dislocations. The diameter of the decohesion core is about 1 nm; the average dislocation spacing is more than 100 nm.

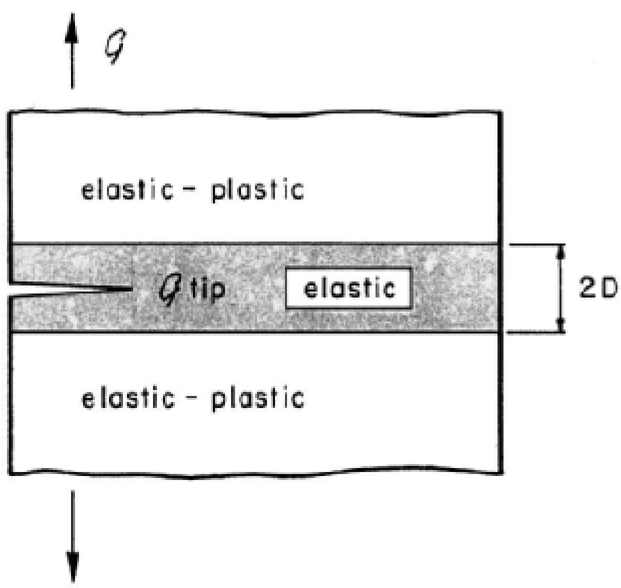

Figure 12.16. A model system with a step-function decay in yield strength.

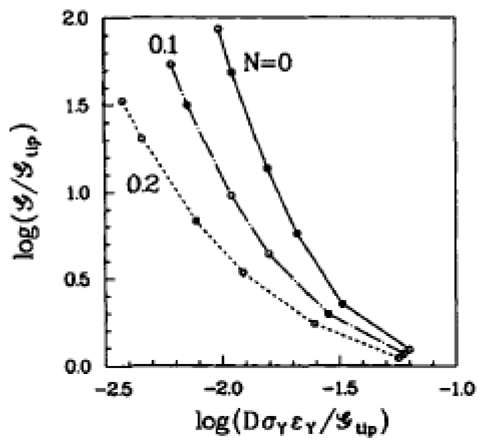

Figure 12.17. A fracture resistance curve: the fracture energy increases as the crack grows. Computed shielding ratio as a function of various parameters: *N*—hardening exponent, *D*—elastic cell size.

Constrained Plasticity

Constrained plasticity. A thin metal film is sandwiched between two elastic substrates. A debond crack preexists on one of the interfaces. The substrates are loaded to open the crack. Let h be the thickness of the metal film thickness, and r_p be the plastic zone size upon crack propagation. When $h \gg r_p$, the substrates place no additional constraint on fracture.

When $h < r_p$, however, the substrates constrain the plastic flow in the film. As the load increases and the crack tip blunts, the level of the peak stress in the metal increases, and the location of the peak stress is several times the film thickness ahead of the crack tip (Varias et al., 1991). The high stress activates flaws ahead of the crack tip into new debond areas, which link back to the main crack (Reimanis et al., 1991).

When the film thickness is very small, the dislocations emitted from the crack tip pile up at the substrate-film interfaces. As the load increases and the crack tip blunts, more dislocations pile up and the stress at the crack tip can increase up to the theoretical strength (Hsia et al., 1994). Even FCC metals can fracture by cleavage this way. This is perhaps an ultimate form of constraint.

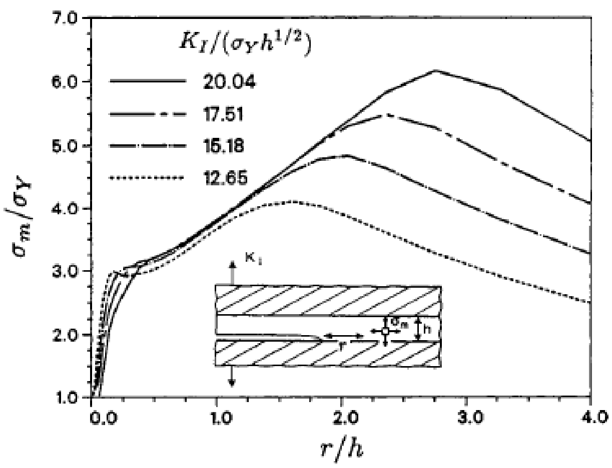

Figure 12.10. Inset: a metal foil bonded between two ceramic substrates, subjected to a remote Mode I stress intensity factor. The mean stress distribution ahead of the crack tip is plotted for several loading levels.

Reviews

A.G. Evans. Perspective on the development of high-toughness ceramics. Journal of American Ceramic Society 73, 187-206 (1990). http://www.ceramics.org/wp-content/uploads/2009/03/evans_high_toughness_ceramics.pdf

Z. Suo and C. F. Shih. Models for metal/ceramic interface fracture. In Metal-Matrix Composites, Ed. S. Suresh, A. Mortensen and A. Needleman, Butterworth-Heinemann, Stoneham, MA. 217-232 (1993). http://www.seas.harvard.edu/suo/papers/033.pdf

J.W. Hutchinson and A.G. Evans. Mechanics of Materials: Top-Down Approaches to Fracture. Acta Materialia 48, 125-135 (2000). http://www.seas.harvard.edu/hutchinson/papers/hutch_mech_of_mater.pdf

J.P. Gong. Why are double network hydrogels so tough? Soft Matter 6, 2583-2590 (2010).

X. Zhao. Multi-scale multi-mechanism design of tough hydrogels: building dissipation into stretchy networks. Soft Matter 10, 672-687 (2014).

A. Pineau, A.A. Benzerga, T. Pardoen. Failure of metals III: Fracture and fatigue of nanostructure metallic materials. Acta Materialia 107, 508-544 (2016).

C. Creton and M. Ciccotti. Fracture and adhesion of soft materials: a review. Reports on Progress in Physics 79, ??-?? (2016).

References

E.H. Andrews. Rupture propagation in hysteresial materials: stress at a notch. Journal of the Mechanics and Physics of Solids 11, 231-242 (1963).

B. Budiansky, J.C. Lambropoulos, J.W. Hutchinson. Continuum Theory of Dilatant Transformation Toughening in Ceramics. International Journal of Solids and Structures 19, 337-355 (1983). http://www.seas.harvard.edu/hutchinson/papers/365.pdf

J. Du, M.D. Thouless and A.F. Yee. Development of a process zone in rubber-modified epoxy polymers. Intrenational Journal of Fracture 92, 271-285 (1998).

R.C. Garvie, R.H. Hannink, R.T. Pascoe. Ceramic steel? Nature 258, 703-704 (1975).
J.P. Gong, Katsuyama, Y., Kurokawa, T. & Osada, Y. Double-network hydrogels with extremely high mechanical strength. Adv. Mater. 15, 1155–1158 (2003).
K.J. Hsia, Z. Suo, and W. Yang. Cleavage due to dislocation confinement in layered materials. J. Mech. Phys. Solids. 42, 877-896 (1994). http://www.seas.harvard.edu/suo/papers/045.pdf
A. Needleman. A continuum model for void nucleation by inclusion debonding. Journal of Applied Mechanics 54, 525-531 (1987).
I.E. Reimanis, B.J. Dalgleish, A.G. Evans. The fracture-sesistance of a model metal ceramic interface. Acta Metallurgica Materialia 39, 3133-3141.
Jeong-Yun Sun, Xuanhe Zhao, Widusha R.K. Illeperuma, Kyu Hwan Oh, David J. Mooney, Joost J. Vlassak, Zhigang Suo. Highly stretchable and tough hydrogels. Nature 489, 133-136 (2012). http://www.seas.harvard.edu/suo/papers/273.pdf
Z. Suo, C.F. Shih, A.G. Varias. A theory for cleavage cracking in the presence of plastic flow. Acta Metallurgica Materialia 41, 1551-1557 (1993). http://www.seas.harvard.edu/suo/papers/032.pdf
V. Tvergaard and J.W. Hutchinson. The relation between crack growth resistance and fracture process parameters in elastic-plastic solids. Journal of the Mechanics and Physics of Solids 40, 1377-1397 (1992). http://www.seas.harvard.edu/hutchinson/papers/420.pdf
A.G. Varias, Z. Suo and C.F. Shih. Ductile failure of a constrained metal foil. Journal of the Mechanics and Physics of Solids 39, 963-986 (1991). http://www.seas.harvard.edu/suo/papers/012.pdf
Y. Wei, J.W. Hutchinson. Models of interface separation accompanied by plastic dissipation at multiple scales. International Journal of Fracture 95, 1-17, (1999). http://www.seas.harvard.edu/hutchinson/papers/Wei_models_of_interface.pdf